Journal of Advanced Research in Fluid Mechanics and Thermal Sciences

Journal homepage:
https://semarakilmu.com.my/journals/index.php/fluid_mechanics_thermal_sciences/index
ISSN: 2289-7879

Saturated Porous Ferroconvection in a Ferrofluid Layer with Viscosity as a Function of Magnetic Field: Focus on Convective Boundary Condition

Rajagopalan Suprabha[1,*], Chikkabagilu Rudraiah Mahesha[1], Chikkanalluru Erappa Nanjundappa[2]

[1] Department of Industrial Engineering and Management, Dr. Ambedkar Institute of Technology, Bengaluru, Visvesvaraya Technological University, Belagavi, India
[2] Department of Mathematics, Dr. Ambedkar Institute of Technology, Bengaluru, Visvesvaraya Technological University, Belagavi, India

ARTICLE INFO

Article history:
Received 8 November 2023
Received in revised form 11 February 2024
Accepted 23 February 2024
Available online 15 March 2024

Keywords:
Ferroconvection; porous medium layer; Galerkin method; MFD viscosity; paramagnetic boundaries

ABSTRACT

The present work aims to examine the influence of magnetic field dependent (MFD) viscosity on the onset of ferroconvection in a horizontal porous layer saturated with a quiescent ferrofluid and subjected to a uniform vertical magnetic field. It is assumed that the porous boundaries at the bottom and top are rigid-paramagnetic. The thermal conditions consist of a constant heat flux at the lower surface and a convective boundary condition at the upper surface, encompassing fixed temperature and uniform heat flux cases. The application of the Galerkin technique to the resulting eigenvalue problem reveals that the stability region expands as the porous parameter, Biot number, MFD viscosity parameter and magnetic susceptibility increase in magnitude. Conversely, the stability region contracts as the magnetic number and non-linearity of magnetization increase. Furthermore, it is noted that under uniform heat flux boundary conditions, the criterion for the initiation of ferroconvection remains unaffected by the non-linearity of fluid magnetization.

1. Introduction

Ferrofluids are versatile materials that have garnered significant attention in recent decades due to their unique properties and wide-ranging applications. An ferrofluids is a colloidal suspension of magnetic nanoparticles, typically iron oxide or cobalt ferrite, stably dispersed in a carrier fluid, often a hydrocarbon-based solvent or water. First developed by NASA in the 1960s for space-related applications, ferrofluids have since found a wide array of applications in engineering, medicine, electronics, and various other fields. Some of the notable applications include magnetic sealing, damping, drug delivery systems, loudspeaker technology and cooling in electronics [1-5].

Numerous research studies have been undertaken to examine the phenomenon of convection in ferrofluids through porous media [6-10]. The ferrofluid’s magnetic properties, the porous material's structure, and outside influences like gravity and a magnetic field all have an impact on the flow patterns and heat transmission characteristics. Qin and Chadam [11] extended the nonlinear stability

* *Corresponding author.*
E-mail address: rsuprabha@yahoo.com

https://doi.org/10.37934/arfmts.115.1.126142

analysis to consider thermal convection in a ferrofluid-saturated porous medium with inertial effects by adopting the Darcy-Forchheimer model. Borglin *et al.,* [12] shown through experimentation that using permanent magnets generated a predictable pressure gradient that induced fluid flow, allowing ferrofluid to be retained in the porous media in predetermined configurations solely determined by the magnetic field. Shivakumara *et al.,* [13] analyzed the impact of vertical permeability heterogeneity on the onset of ferroconvection in a horizontal layer of magnetized Darcy porous media that is saturated with ferrofluid for various permeability function forms. Nanjundappa *et al.,* [14] elucidated the influence of cubic temperature profiles on the initiation of ferroconvection in a Brinkman porous medium under a uniform vertical magnetic field. Control volume based finite element method was employed by Li *et al.,* [15] to simulate ferrofluid migration due to magnetic forces in a porous cylinder using a single-phase model to predict nanofluid characteristics. Siddiqui and Turkyilmazoglu [16] employed the modified Rosensweig-model to numerically investigate heat transfer in a water-based ferrofluid enclosed porous cavity with a novel permeable chamber using the successive-overrelaxation method (SOR). A linear stability analysis was conducted by Senin *et al.,* [17] to examine how internal heating and variable gravity in an anisotropic porous medium affect the initiation of Benard-Marangoni convection in a ferrofluid layer system. Nanjundappa *et al.,* [18] investigated theoretically the penetrative ferro-thermal-convection (FTC) via internal heating in a ferrofluid-saturated porous layer for different types of velocity, temperature and magnetic potential bounding surfaces. Saeed *et al.,* [19] employed the RK4 shooting method to investigate the influence of temperature-dependent viscosity (TDV) and thermal conductivity on ferrofluid (FF) flow through a porous medium adjacent to a vertically stretching surface. The initial flow of immiscible fluids in a porous medium subjected to a rapid pressure gradient and a transverse magnetic field was studied by Goyal and Srinivas [20] to explore the influence of Hartmann number and porous medium parameters on the system's physical characteristics.

In ferrofluid saturating a porous media, Sunil and Sharma [21] studied the effect of MFD viscosity on thermo--solutal convection, taking into account a fluid layer heated and soluted from below in the presence of a uniform magnetic field with two free boundaries. Nanjundappa *et al.,* [22] investigated the impact of MFD viscosity on the initiation of Bénard–Marangoni ferroconvection with rigid-free boundaries to obtain the critical stability parameters using the Rayleigh–Ritz method. Bhandari [23] analyzed the influence of MFD viscosity on ferrofluid flow around a rotating disk in the existence of a stationary magnetic field using the Neruinger-Rosensweig model and solving the nonlinear coupled equations with Flex PDE. Molana *et al.,* [24] examined the natural convection heat transfer of Fe_3O_4-water nanofluids with MFD viscosity in a unique porous cavity geometry under a constant inclined magnetic field. The impact of a perpendicular magnetic field on the flow of micropolar nanofluid over an impermeable stretching sheet in a porous medium and the combined convection heat transfer was investigated by Izadi *et al.,* [25] in relation to the control of MFD viscosity. Savitha *et al.,* [26] examined the impact of viscosity at MFD and energy-based volumetric internal heating in conjunction involving ferrofluid-saturated porous layers on convection Robin-type thermal and magnetic potential boundary conditions.

Each of the aforementioned investigations has focused on isothermal boundary conditions at the ferrofluid layer's surfaces. In spite of this, these conditions might prove to be overly restrictive when actual situations are taken into account. Hence, the purpose of this research is to investigate the impact of MFD viscosity on Brinkman-Bénard ferroconvection while relaxing the temperature boundary conditions. This is accomplished by assuming a rigid-paramagnetic lower surface with a constant heat flux and a general type of boundary condition on the upper rigid-paramagnetic boundary. The solution to the subsequent eigenvalue problem is numerically determined using the Galerkin method with second-order Chebyshev polynomials as trial functions.

2. Mathematical Formulation

The system investigated comprises of a horizontal layer of porous medium which is saturated with ferrofluid which is initially quiescent and has an applied vertical magnetic field (H_0). The physical configuration is depicted in Figure 1. The porous layer thickness d between the two surfaces and edge effects are neglected due to its large horizontal extension. The bottom surface of the porous layer serves as the origin of the Cartesian coordinate system (x, y, z) used, and gravity operates in the negative z-direction, $\vec{g} = -g\,\hat{k}$, represented by the unit vector $\hat{k}$. Notably, experimental evidence by Rosensweig *et al.,* [27] has shown that the viscosity of ferrofluids exhibits significant variations with respect to the applied magnetic field. As an initial approximation, the assumption is that the viscosity changes linearly with the magnetic field in the approach, $\eta = \eta_0(1+\vec{\delta}\cdot\vec{B})$, where η is the magnetic viscosity, $\vec{\delta}$ is the coefficient of variation of the MFD viscosity, which is assumed to be independent of the location (i.e., $\delta_x = \delta_y = \delta_z = \delta$), while η_0 represents the ferrofluid's viscosity in the absence of the magnetic field and $\vec{B}$ is the magnetic induction. Additionally, the fluid is considered to be incompressible, and its density variation, following the Boussinesq approximation, can be expressed as

$$\rho = \rho_0[1-\alpha_t(T-T_0)] \tag{1}$$

where ρ is the fluid density, T is the Temperature, T_0 is the lower boundary's temperature, α_t is the thermal expansion coefficient and ρ_0 is the reference density at temperature T_0.

A condition of the type for a constant heat flux exists at the lower surface $(z=0)$ is

$$-k_1\frac{\partial T}{\partial z} = q_0 \tag{2}$$

where k_1 is the thermal conductivity, q_0 is the conductive thermal flux.

Utilizing a general thermal boundary condition at the upper surface $(z=d)$ of the form

$$-k_1\frac{\partial T}{\partial z} = h_t(T-T_\infty) \tag{3}$$

where h_t is heat transfer coefficient and T_∞ is temperature in the bulk of the environment.

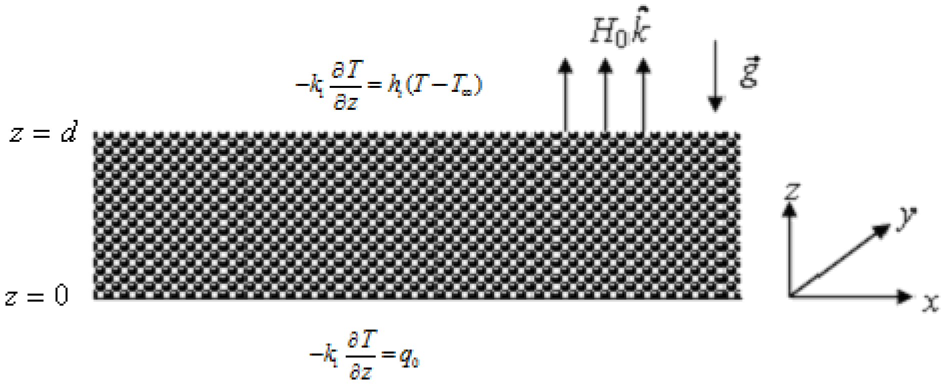

Fig. 1. Physical configuration

The governing equations of continuity, momentum, energy and Maxwell equations respectively are given by Eq. (4)-(7) respectively.

$$\nabla\cdot\vec{q} = 0 \tag{4}$$

$$\rho_0\left[\frac{1}{\varepsilon}\frac{\partial\vec{q}}{\partial t} + \frac{1}{\varepsilon^2}(\vec{q}.\nabla)\vec{q}\right] = -\nabla\mathrm{p} + \rho\,\vec{g} - \frac{\eta}{k}\vec{q} + 2\nabla\cdot(\eta\,\underline{\underline{D}}) + \rho_0(\vec{M}\cdot\nabla)\vec{H} \tag{5}$$

$$\varepsilon\left[\rho_0 C_{V,H} - \mu_0\vec{H}\cdot\left(\frac{\partial\vec{M}}{\partial T}\right)_{V,H}\right]\frac{DT}{Dt} + (1-\varepsilon)(\rho_0 C)_s\frac{\partial T}{\partial t} + \mu_0 T\left(\frac{\partial\vec{M}}{\partial T}\right)_{V,H}\cdot\frac{D\vec{H}}{Dt} = k_1\nabla^2 T \tag{6}$$

$$\nabla\cdot\vec{B} = 0,\ \ \nabla\times\vec{H} = 0\ \ \text{or}\ \vec{H} = \nabla\varphi \tag{7}$$

where $\vec{q} = (u, v, w)$ is velocity vector, p is the pressure, ε is the porosity of the porous medium, t is the time, k is the permeability of the porous medium, $\underline{\underline{D}} = [\nabla\vec{q} + (\nabla\vec{q})^T]/2$ is the rate of strain tensor, $\vec{M}$ is Magnetization, $\vec{H}$ magnetic field's strength, $C_{V,H}$ is the specific heat at constant volume and magnetic field, φ is the magnetic potential, while the subscript s denotes the porous media.

Further, $\vec{B}$, $\vec{M}$ and $\vec{H}$ are related by

$$\vec{B} = \mu_0\left(\vec{M} + \vec{H}\right) \tag{8}$$

with

$$\vec{M} = \frac{\vec{H}}{H}M\left(H, T\right). \tag{9}$$

Eq. (10) denotes the linearized magnetic equation of state with respect to H_0 and T_0

$$M = M_0 + \chi\left(H - H_0\right) - K\left(T - T_0\right) \tag{10}$$

where μ_0 is the vacuum's free space magnetic permeability, χ is the magnetic susceptibility and K is the pyromagnetic co-efficient.

The initial state is considered to be at rest and can be described by the following expression:

$$\vec{q}_b = 0,\ \rho = \rho_b(z),\ \eta = \eta_b(z),\ p = p_b(z),\ T = T_b(z),\ \vec{H} = \vec{H}_b(z),\ \vec{M} = \vec{M}_b(z) \tag{11}$$

where subscript b denotes the basic state.

Using Eq. (11), Eq. (5) and Eq. (6), respectively, yield

$$\frac{dp_b}{dz} = -\rho_0\left[1-\alpha_t\left(T_b - T_0\right)\right] g\,\hat{k} + \mu_0 M_b \frac{dH_b}{dz} \tag{12}$$

$$\frac{d^2 T_b}{dz^2} = 0 \tag{13}$$

Upon solving Eq. (13) with consideration of the boundary conditions of Eq. (2) and Eq. (3), the result obtained is as follows:

$$T_b(z) = -\beta z + \frac{q_0}{h_t} + T_\infty + \beta d \tag{14}$$

where $\beta = q_0 / k_1$ is the temperature gradient.

Upon substituting the basic state Eq. (11) into Eq. (7) and utilizing Eq. (8) and Eq. (10), the magnetic field intensity and magnetization for the basic state is determined as demonstrated in Finlayson [28].

$$\vec{H}_b(z) = \left[H_0 - \frac{K\beta z}{1+\chi}\right]\hat{k} \tag{15}$$

$$\vec{M}_b(z) = \left[M_0 + \frac{K\beta z}{1+\chi}\right]\hat{k} \tag{16}$$

where $M_0 + H_0 = H_0^{ext}$.

Using Eq. (12) to Eq. (14) in Eq. (10) and integrating, we obtain

$$p_b(z) = p_0 - \rho_0 g\, z - \frac{1}{2}\rho_0\alpha_t g\beta z^2 - \frac{\mu_0 M_0 \kappa\beta}{1+\chi} z - \frac{\mu_0\kappa^2\beta^2}{2(1+\chi)^2} z^2 \tag{17}$$

To investigate the system's stability, a small disturbance is applied to the system, and the variables are perturbed in the form:

$$\vec{q} = \vec{q}',\ p = p_b(z) + p',\ \eta = \eta_b(z) + \eta',\ T = T_b(z) + T',\ \vec{H} = \vec{H}_b(z) + \vec{H}',\ \vec{M} = \vec{M}_b(z) + \vec{M}' \tag{18}$$

The perturbed variables $\vec{q}'$, p', η', T', $\vec{H}'$ and $\vec{M}'$ are assumed to be negligible. Eq. (17) is substituted into Eq. (8) and Eq. (9), and Eq. (7) is used and ignoring the primes in the notation,

$$H_x + M_x = \left(1 + \frac{M_0}{H_0}\right) H_x,\ H_y + M_y = \left(1 + \frac{M_0}{H_0}\right) H_y,\ H_z + M_z = (1+\chi)\ H_z - K\ T \tag{19}$$

The above equations are derived under the assumption that $K\beta\, d << (1+\chi)\ H_0$. Substituting the perturbation Eq. (18) into momentum Eq. (5) and linearizing, we obtain (after neglecting the primes)

$$\rho_0 \frac{\partial u}{\partial t} = -\frac{\partial p}{\partial x} - \frac{\eta_b}{k} u + \eta_b \nabla^2 u + \mu_0 (M_0 + H_0) \nabla^2 u + \frac{\partial H_x}{\partial z} \tag{20}$$

$$\rho_0 \frac{\partial v}{\partial t} = -\frac{\partial p}{\partial y} - \frac{\eta_b}{k} v + \eta_b \nabla^2 v + \mu_0 (M_0 + H_0) \nabla^2 v + \frac{\partial H_y}{\partial z} \tag{21}$$

$$\rho_0 \frac{\partial w}{\partial t} = -\frac{\partial p}{\partial z} - \frac{\eta_b}{k} w + \eta_b \nabla^2 w + \mu_0 (M_0 + H_0) \nabla^2 w + \frac{\partial H_z}{\partial z} + \rho_0 \alpha_t g T - \mu_0 K \beta H_z + \frac{\mu_0 K^2 \beta T}{1+\chi} \tag{22}$$

where $\eta_b = \eta_0 [1 + \delta\, \mu_0 (M_0 + H_0)]$ and $\nabla^2 = \partial^2/\partial x^2 + \partial^2/\partial y^2 + \partial^2/\partial z^2$ is the Laplacian operator.

Eq. (20) and Eq. (21) can be partially differentiated with respect to *x* and *y*, respectively, and added, we obtain

$$\nabla_h^2 p = \rho_0 \frac{\partial}{\partial z}\left(\frac{\partial w}{\partial t}\right) + \frac{\eta_b}{k} \frac{\partial w}{\partial z} - \eta_b \frac{\partial}{\partial z}\left(\nabla^2 w\right) + \mu_0 (M_0 + H_0) \frac{\partial}{\partial z}\left(\frac{\partial H_x}{\partial x} + \frac{\partial H_y}{\partial y}\right) \tag{23}$$

where $\nabla_h^2 = \partial^2/\partial x^2 + \partial^2/\partial y^2$ is the horizontal Laplacian operator

Eq. (22) is simplified by substituting Eq. (23) to eliminate the pressure term, we obtain

$$\left(\rho_0 \frac{\partial}{\partial t} + \frac{\eta_b}{k} - \eta_b \nabla^2\right) \nabla^2 w = -\mu_0 K \beta \frac{\partial}{\partial z}\left(\nabla_h^2 \varphi\right) + \frac{\mu_0 K^2 \beta}{1+\chi} \nabla_h^2 T + \rho_0 \alpha_t g \nabla_h^2 T \tag{24}$$

As before, substituting Eq. (18) into Eq. (6), linearizing and the resulting equation upon using $\vec{H} = \nabla \varphi$, we obtain (after neglecting primes)

$$(\rho_0 C)_1 \frac{\partial T}{\partial t} - \mu_0 T_0 K \frac{\partial}{\partial t}\left(\frac{\partial \varphi}{\partial z}\right) = k_1 \nabla^2 T + \left[(\rho_0 C)_2 - \frac{\mu_0 T_0 K^2}{1+\chi}\right] w \beta \tag{25}$$

where $(\rho_0 C)_1 = \varepsilon\, \rho_0 C_{V,H} + \varepsilon\, \mu_0 H_0 K + (1-\varepsilon)(\rho_0 C)_s$ and $(\rho_0 C)_2 = \varepsilon\, \rho_0 C_{V,H} + \varepsilon\, \mu_0 H_0 K$.

After substituting Eq. (18) and using Eq. (19), Eq. (7) can be rewritten (omitting the primes) as

$$\left(1+\frac{M_0}{H_0}\right)\nabla_h^2\varphi+\left(1+\chi\right)\frac{\partial^2\varphi}{\partial z^2}-K\frac{\partial T}{\partial z}=0 \tag{26}$$

It is expected that the dependent variables' normal mode expansion will have the form

$$\left\{w,T,\varphi\right\}=\left\{W(z),\Theta(z),\Phi(z)\right\}\exp\left[i(\ell x+my)+\omega t\right] \tag{27}$$

where W, Θ and Φ are the amplitudes of the perturbed vertical component velocity, temperature and magnetic potential respectively, while ω is the growth rate and ℓ, m are the wave numbers in the x and y directions.

After substituting normal mode expansion Eq. (27) into Eq. (24) to Eq. (26) and then all the variables are non-dimensionalized using the following relations

$$z^*=\frac{z}{d},\quad W^*=\frac{d}{\nu A}W,\quad t^*=\frac{\nu}{d^2}t,\quad \omega^*=\frac{d^2}{\nu}\omega,\quad \Theta^*=\frac{\kappa}{\beta\nu d}\Theta,$$

$$\Phi^*=\frac{(1+\chi)\ \kappa}{\mathrm{K}\,\beta\nu d^2}\ \Phi\ \text{ and }\ \delta^*=\mu_0(M_0+H_0)\delta \tag{28}$$

where $\nu=\eta_0/\rho_0$ is the kinematic viscosity, $A=(\rho_0 C)_1/(\rho_0 C)_2$ is the heat capacity ratio and $\kappa=k_1/(\rho_0 C)_2$ is the thermal diffusivity.

To obtain the ordinary differential equations of the form (omitting the asterisks),

$$\left[(1+\delta)\left\{(D^2-a^2)-\sigma^2\right\}-\omega\right](D^2-a^2)W=-a^2\left[N\,D\Phi-\left(R+N\right)\Theta\right] \tag{29}$$

$$\left(D^2-a^2-\Pr\omega\right)\Theta-\Pr M_2\omega D\Phi=-\left(1-M_2A\right)W \tag{30}$$

$$\left(D^2-a^2M_3\right)\Phi=D\Theta \tag{31}$$

where $D=d/dz$ is differential operator, $a=\sqrt{l^2+m^2}$ is the horizontal wave number, $\sigma^2=d/\sqrt{k}$ is the porous parameter, $R=\alpha_t g\beta d^4/\nu\kappa A$ is the thermal Rayleigh number, $M_1=\mu_0K^2\beta/(1+\chi)\alpha_t\rho_0 g$ is the magnetic number, $N=RM_1=\mu_0K^2\beta^2d^4/(1+\chi)\,\eta_0\,\kappa A$ is the magnetic Rayleigh number, $\Pr=\nu/\kappa$ is the Prandtl number, $M_2=\mu_0T^2K^2/(1+\chi)(\rho_0C)_s$ is the magnetic parameter, $M_3=(1+M_0/H_0)/(1+\chi)$ is the Magnetization parameter's nonlinearity.

Owing to its average value for ferrofluid with various carrier liquids, which is of the order of 10^{-6}, the effect of M_2 is ignored in comparison to unity [28].

The ordinary differential Eq. (29) to Eq. (31) are solved using the following boundary conditions

$$W=DW=(1+\chi)D\Phi-a\Phi=D\Theta=0\ \text{ at }\ z=0\quad \text{(on the lower rigid-paramagnetic)} \tag{32}$$

$$W = DW = (1+\chi)D\Phi + a\Phi = D\Theta + Bi\,\Theta = 0 \text{ at } z=1 \text{ (at the upper rigid-paramagnetic)} \tag{33}$$

The case $Bi = 0$ and $Bi \to \infty$ to upper boundary conditions with constant heat flux and temperature, respectively.

3. Method of Solution

Considering the validity of the principle of exchange of stability, we set $\omega = 0$ in Eq. (29) to Eq. (31) and simplifying, we get

$$\left[(1+\delta)(D^2 - a^2 - \sigma^2)\right](D^2 - a^2)W = -a^2 R\left[M_1 D\Phi - (1+M_1)\Theta\right] \tag{34}$$

$$(D^2 - a^2)\Theta = -W \tag{35}$$

$$(D^2 - a^2 M_3)\Phi - D\Theta = 0 \tag{36}$$

The eigenvalue problem, consisting of Eq. (29) to Eq. (31) along with the selected boundary conditions Eq. (32) and Eq. (33), is mathematically resolved using the Galerkin Method to obtain *R* as the eigenvalue. Consequently, W, Θ and Φ are expressed as follows.

$$W = \sum_{i=1}^{n} A_i W_i(z), \quad \Theta(z) = \sum_{i=1}^{n} C_i\ \Theta_i(z), \quad \Phi(z) = \sum_{i=1}^{n} D_i\ \Phi_i(z) \tag{37}$$

The unknown constants, A_i, C_i and D_i are determined through the chosen base functions $W_i(z)$, $\Theta_i(z)$ and $\Phi_i(z)$, which are generally selected to satisfy the corresponding boundary conditions. After substituting Eq. (37) into Eq. (34) to Eq. (36), the resulting equations are respectively multiplied with $W_j(z)$, $\Theta_j(z)$ and $\Phi_j(z)$. The equations obtained are subsequently integrated by parts between the lower and upper limits of z i.e., $(0,\ 1)$ and are evaluated using boundary conditions. The resulting equations constitute a system of linear homogeneous algebraic equations:

$$C_{ji}A_i + D_{ji}C_i + E_{ji}D_i = 0 \tag{38}$$

$$F_{ji}A_i + G_{ji}C_i = 0 \tag{39}$$

$$H_{ji}C_i + I_{ji}D_i = 0\,. \tag{40}$$

The inner products of the basic functions are involved in the coefficients $C_{ji} - I_{ji}$, which are provided by

$$C_{ji} = (1+\delta)[< D^2W_j D^2W_i > + (2a^2 + \sigma^2) < DW_j DW_i > + a^2(a^2 + \sigma^2) < W_j W_i >]$$
$$D_{ji} = -a^2 R(1+M_1) < W_j\ \Theta_i >$$
$$E_{ji} = a^2 R M_1 < W_j D\Phi_i >$$

$$F_{ji} = -<\Theta_j W_i>$$
$$G_{ji} = Bi\,\Theta_j(1)\Theta_i(1) + <D\Theta_j D\Theta_i> + a^2 <\Theta_j \Theta_i>$$
$$H_{ji} = -<D\Phi_j \Theta_i>$$
$$I_{ji} = \frac{a}{1+\chi}\left[\Phi_j(1)\Phi_i(1) + \Phi_j(0)\Phi_i(0)\right] + <D\Phi_j D\Phi_i> + a^2 M_3 <\Phi_j \Phi_i>$$

where $<\cdots> = \int_0^1 (\cdots)\,dz$ is the specification of the inner product.

There is a non-trivial solution to the set of homogeneous algebraic equations stated above if and only if

$$\begin{vmatrix} C_{ji} & D_{ji} & E_{ji} \\ F_{ji} & G_{ji} & 0 \\ 0 & H_{ji} & I_{ji} \end{vmatrix} = 0. \tag{41}$$

The extraction of eigenvalues from Eq. (41) is done by selecting the trial functions as

$$W_i = (z^4 - 2z^3 + z^2)T_{i-1}^*, \quad \Theta_i = z^2(1-2z/3)T_{i-1}^*, \quad \Phi_i = (z-1/2)T_{i-1}^* \tag{42}$$

In the process of solving the eigenvalue problem, trial functions are used to approximate the solutions for the dependent variables W_i, Θ_i and Φ_i. These trial functions are represented by the modified Chebyshev polynomials, denoted as $T_i^*\,'s.$ However, these trial functions may not satisfy the boundary conditions initially. To address this, the residual technique is employed. The residual term, which appears as the first term on the right-hand side of the characteristic equations G_{ji} and I_{ji}, accounts for the deviation of the trial functions from the actual boundary conditions. By incorporating this residual term, the characteristic equation can accurately describe the behavior of the system. The extracted eigenvalue determines the stability of the system and provide crucial information about the convection behavior of the ferrofluids flowing through porous media under the influence of a magnetic field.

Eq. (41) allows for the derivation of a relation with the characteristic parameters of the following type

$$f(R,\, \delta,\, \sigma^2,\, Bi,\, N,\, M_1,\, M_3,\, a) = 0 \tag{43}$$

Numerical analysis is utilized to determine the critical value of R, $(i.e., R_c)$ corresponding to various values of wave number a by varying it for different δ, N, σ^2, Bi, M_1 and M_3.

4. Results

The effect of MFD viscosity on the initiation of Brinkman-Benard ferroconvection in a horizontal ferrofluid-saturated porous layer under the influence of a uniform vertical magnetic field is examined. The analysis is conducted using linear stability theory. In order to establish the rigid-paramagnetic nature of the upper and lower boundaries of the porous layer, a general thermal condition is applied to the upper boundary and a uniform heat flux condition is applied to the lower boundary. Numerically, the eigenvalue problem that results is resolved by employing the Galerkin method. Initially, we verify the numerical method employed through a comparison of the critical Rayleigh number (R_c) and the corresponding critical wave number (a_c) with the values reported by Sparrow *et al.,* [29] for a conventional viscous fluid. It has been noted that in order to achieve convergent results, six terms $(n = 6)$ are necessary in the series expansion of Eq. (37). A comparison between our findings and those of Sparrow *et al.,* [29] for different Biot numbers (Bi) in the limiting case of $M_1 = 0$, $M_3 = 0$, $\sigma = 0$ and $\delta = 0$ (i.e., ordinary viscous fluid) is presented in Table 1. The correctness of the numerical process used to identify the essential stability parameters is confirmed by the good agreement between the two methods.

Table 1
R_c and a_c comparison for various Bi

Bi	Sparrow *et al.,* [29]		Present analysis	
	Rigid- Rigid		Rigid-Rigid	
	R_c	a_c	R_c	a_c
0	720. 000	0.00	720.000	0.000
0.01	747.765	0.71	747.765	0.7126
0.03	768.153	0.93	768.155	0.9283
0.1	807.676	1.23	807.676	1.2281
0.3	869.231	1.57	869.208	1.5571
1	974.173	1.94	974.172	1.9427
3	1093.744	2.24	1093.74	1.2419
10	1204.571	2.44	1204.57	2.4367
30	1259.884	2.51	1259.91	2.5110
100	1284.263	2.53	1284.28	2.5394
∞	1295.781	2.55	1295.78	2.5490

The value of R_c by corresponding the wave numbers a_c obtained for different physical parameters $\delta,\ \sigma^2,\ N,\ Bi$, M_1, M_3 and χ are presented graphically in Figure 2 to Figure 6. The effect of the Biot number (Bi) on the critical Rayleigh number (R_c) is studied while considering the variation of MFD viscosity in the context of Brinkman-Benard ferroconvection in Figure 2. Assigned to the boundary of the porous medium, the Biot number quantifies the relationship between the internal thermal resistance of the solid matrix and the external thermal resistance at the boundary of the porous medium. The initiation of convection in such systems is significantly influenced by it. The variation of critical Rayleigh number R_c and wave number a_c is shown in Figure 2(a) and Figure 2(b) respectively as a function of MFD viscosity parameter δ for different Bi and χ when $M_3 = 1$, $M_1 = 5$ and $\sigma^2 = 50$. Figure 2(a) illustrates that R_c increases with an increment in MFD viscosity parameter (δ), resulting in a stabilizing effect and delaying the onset of ferroconvection. Additionally, the variation in Bi from 0 *to* 2 significantly impacts the critical Rayleigh number, R_c with the most stable condition observed for $Bi = 0$ and the least stable for $Bi = 2$, as the system changes from an insulated to a conductive upper boundary. Moreover, the system exhibits higher stability with paramagnetic boundaries having large susceptibility $(1+\chi = 10^4)$ compared to $\chi = 0$, although the control of magnetic susceptibility diminishes as χ increases. This finding aligns with the results obtained by Gotoh and Yamada [30]. On the other hand, Figure 2(b) demonstrates that an increase in Bi and χ leads to an increase in the critical wave number (a_c), reducing the size of convection cells, while δ does not affect the critical wavenumber. This behavior holds the initiative that higher values of Bi lead to enhanced thermal conductivity within the porous medium, allowing heat to be transported more efficiently. As the magnetic susceptibility increases, the ferrofluid becomes more responsive to the magnetic field, leading to stronger magnetization effects. This enhanced magnetization creates stronger interactions between magnetic particles in the fluid, affecting its flow behavior. The increased magnetic response results in a more stable system, requiring higher convective instability (higher critical Rayleigh number) to trigger convection.

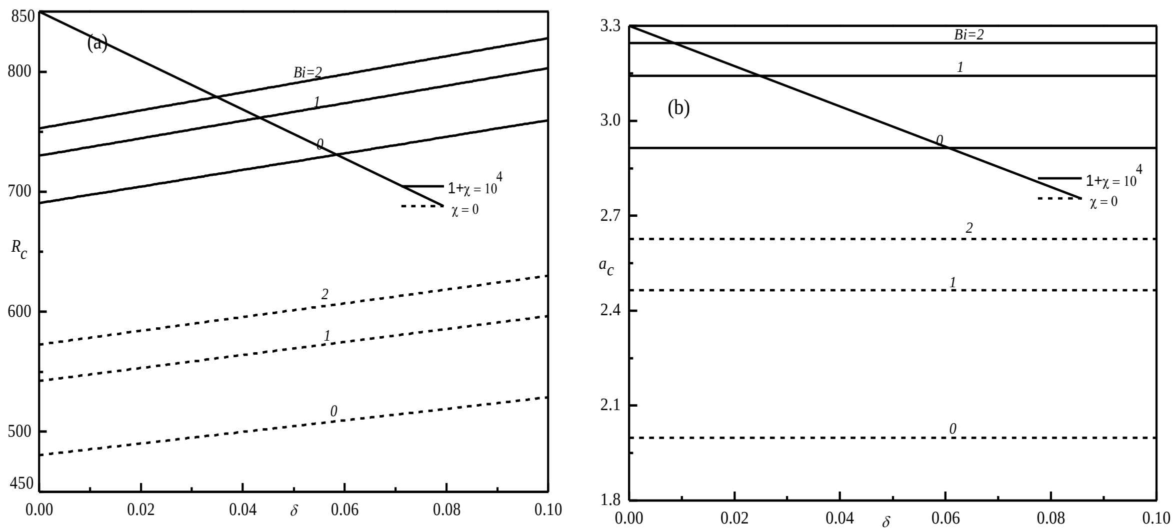

Fig. 2. Variation of (a) R_c and (b) a_c with δ for different Bi and χ for $M_3 = 1$, $M_1 = 5$ and $\sigma^2 = 50$

Figure 3(a) and Figure 3(b) display the variation of R_c and a_c respectively, as a function of MFD viscosity δ to examine the influence of the porous medium's coarseness on the onset of ferroconvection for different values of σ^2 and χ with fixed values of $M_1 = 5$, $M_3 = 1$ and $Bi = 2$. When the porous parameter σ^2 increases for a fixed thickness of the porous layer, it leads to a decrease in the permeability of the porous medium. This behavior can be attributed to the decreased fluid flow caused by a larger porous parameter σ^2, which hinders the convective heat transfer within the system. The reduced flow velocities restrict the transport of heat and result in less efficient mixing of the fluid, delaying the onset of ferroconvection. Thus, it requires higher heating and a higher value of the thermal Rayleigh number for the onset of ferroconvection in the ferrofluid-saturated porous medium. Figure 3(b) demonstrates that in the absence of the pyromagnetic coefficient $(\chi = 0)$, an increase in σ^2 causes cell size a_c to become destabilizing. However, for a high pyromagnetic coefficient $(1+\chi = 10^4)$ an increase in σ^2 results in a stabilizing nature of cell size a_c.

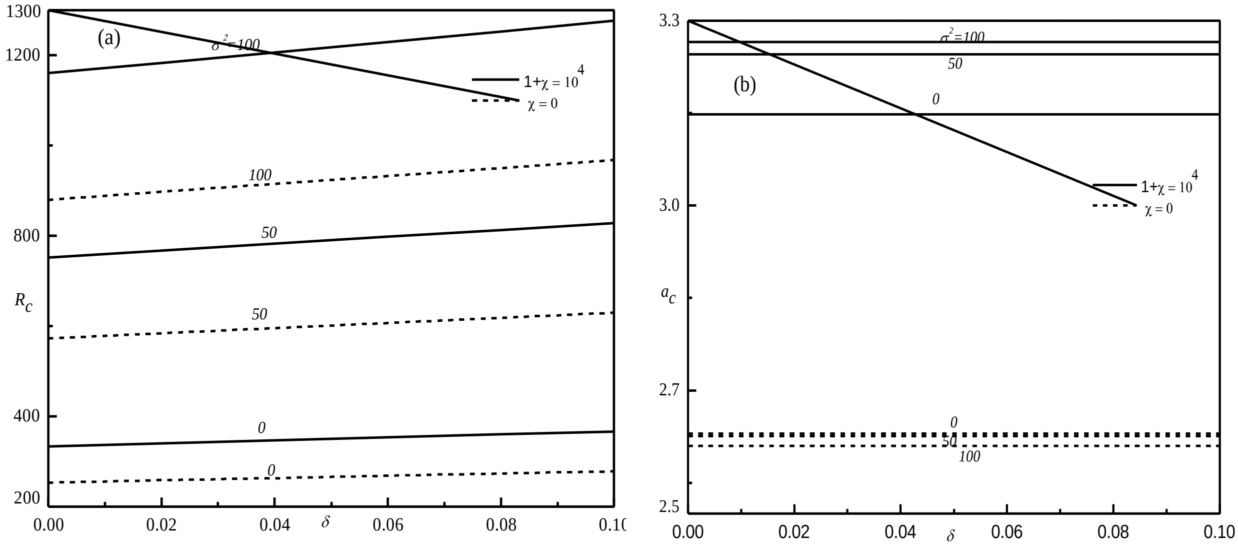

Fig. 3. Variation of (a) R_c and (b) a_c with δ for different values of σ^2 and χ for $M_3=1,\ M_1=5,\ Bi=2$

By plotting the critical Rayleigh number R_c against the MFD viscosity parameter δ, Figure 4(a) illustrates the influence of the magnetic number M_1 on the initiation of ferroconvection for $M_3=1$, $\sigma^2=50$ and $Bi=2$. The magnetic number (M_1) is a dimensionless parameter that characterizes the relative strength of the magnetic forces to buoyancy forces in a ferrofluid system. When the magnetic number is increased, it implies that the magnetic forces become more dominant compared to buoyancy forces. An increase in the magnetic number is observed to have a destabilizing effect. This pattern can be explained by attributing it to the enhanced magnetic response of the ferrofluid as the magnetic number increases. The stronger magnetic forces lead to more vigorous fluid motion and heat transfer, promoting convection at lower thermal gradients. The stronger magnetic field enhances the interaction between magnetic particles in the ferrofluid, leading to more significant disturbances and convection. On the other hand, a lower magnetic number would result in a more stable system with smaller and less pronounced convection cells. The observed trend in Figure 4(b) reveals that with an increase in the magnetic number (M_1), the critical wave number (a_c) also increases, leading to a reduction in the size of convection cells. This implies that as the magnetic field strength increases, the convection cells become smaller and more compact, indicating a more organized and stable flow pattern within the ferrofluid-saturated porous layer.

Figure 5(a) illustrates the impact of the nonlinearity of fluid magnetization (M_3) on the onset of ferroconvection. The curves of R_c versus δ are shown for different M_3 and χ when $\sigma^2=50$, $M_1=5$ and $Bi=2$. The non-linearity of fluid magnetization refers to the deviation of the magnetic response of ferrofluid from a simple linear relationship with the applied magnetic field. In ferrofluids, the magnetization is often dependent on both the magnitude of the magnetic field and the temperature, resulting in non-linear behavior. The pyromagnetic coefficient quantifies the rate at which the magnetization changes with temperature. The graph demonstrates that an increase in M_3 has a destabilizing effect on the system, making it more prone to convection. However, the destabilization caused by M_3 is relatively small. This can be explained by the fact that when the pyromagnetic coefficient is large, the magnetization becomes highly dependent on temperature, making it more non-linear. This non-linearity of magnetization has significant implications for the behavior of the ferrofluid in response to external magnetic fields and thermal gradients, which accelerates the initiation of convection due to a reduction in stability region. Similar patterns of behavior are seen in the case of critical wave numbers, as shown in Figure 5(b), where an increase in M_3 causes a decrease in a_c and a resulting increase in convection cell size.

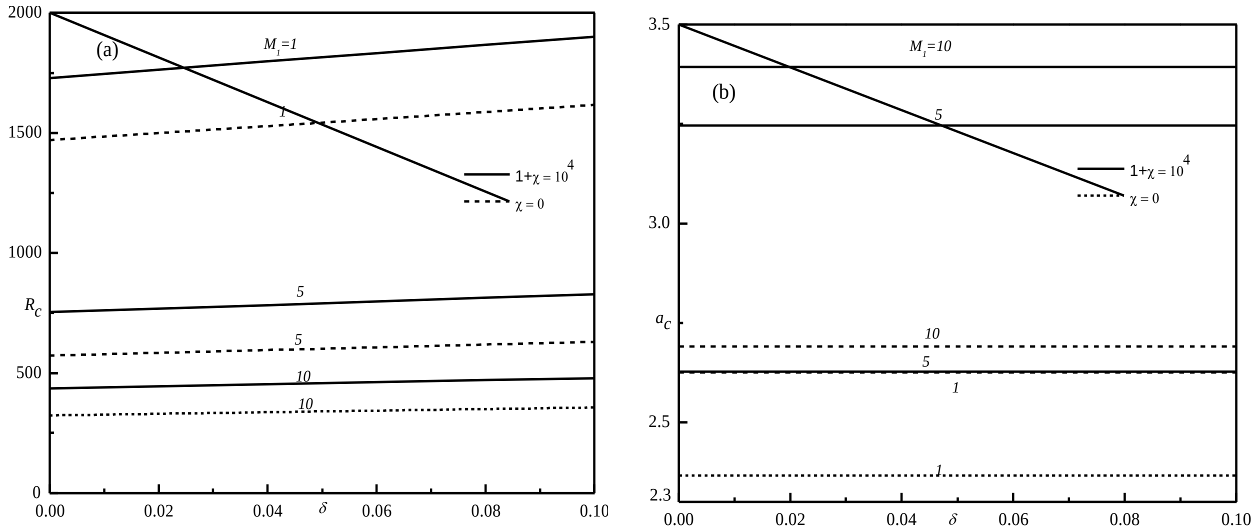

Fig. 4. Variation of (a) R_c and (b) a_c as a function of δ for different M_1 and χ for $M_3 = 1,\ \sigma^2 = 50,\ Bi = 2$

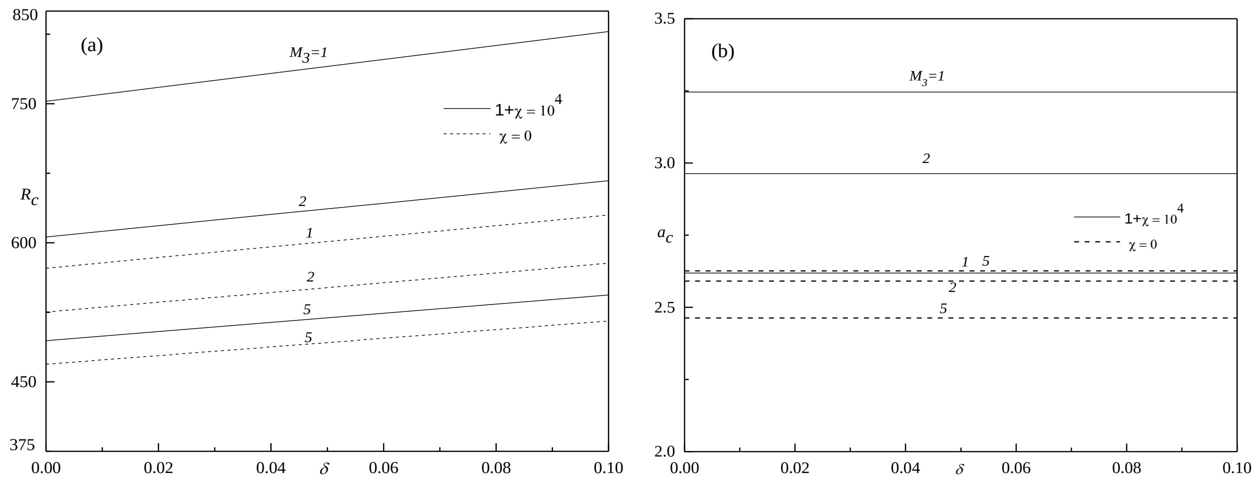

Fig. 5. Variation of (a) R_c and (b) a_c as a function δ for different M_3 and χ for $M_1 = 5,\ \sigma^2 = 50,\ Bi = 2$

The combined influence of buoyancy and magnetic forces is depicted in Figure 6 through the locus of R_c and $N_c\left(N_c = R_c M_1\right)$ for various M_3 and χ when $\sigma^2 = 50$, $\delta = 0.02$ and $Bi = 2$. The relationship between R_c and N_c is inversely proportional. For $M_3 \to \infty$ case, the data aligns with the correlation

$$\frac{R_c}{R_{c0}} + \frac{N_c}{N_{c0}} = 1$$

as observed in the non-porous case for constant viscosity ferrofluids [28, 30]. Here, R_{c0} is the critical thermal Rayleigh number without magnetic field $(N = 0)$ and N_{c0} is the critical magnetic Rayleigh number in the absence of gravity $(R = 0)$.

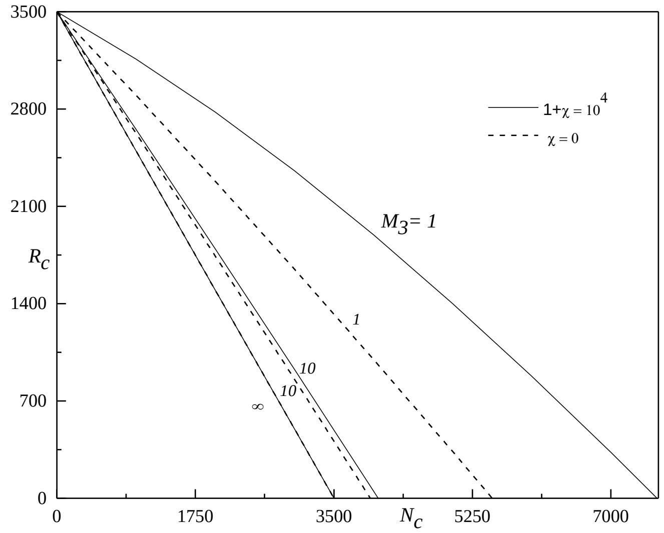

Fig. 6. Variation of R_c verses N_c for different M_3 and χ for $\delta =$ 0.02, $\sigma^2 = 50$ and $Bi = 2$

The values of the critical stabilities parameters R_c and N_c are tabulated for different values of δ, Bi, σ, M_3 and χ in Table 2 to 4. From the tables, it is evident that R_c and N_c are increasing as a function of MFD viscosity parameter δ. In the scenario of negligible buoyancy (i.e., $R = 0$), it is observed that the critical magnetic Rayleigh number N_c decreases as M_3 increases. These findings indicate that the ferrofluid-saturated porous layer becomes more susceptible to temperature gradients when influenced by magnetic forces and/or greater non-linearity of the fluid magnetization. As M_3 approaches to infinity, the results converge towards those of the classical Bénard problem, consistent across various magnetic susceptibility values.

Table 2
Variation of R_c and N_c for different δ, M_3 and χ when $Bi = \sigma = 0$

δ	R_c ($N = 0$)	N_c ($R = 0$)					
		$M_3 = 1$		$M_3 = 10$		$M_3 \to \infty$	
		$\chi = 0$	$\chi = 9999$	$\chi = 0$	$\chi = 9999$	$\chi = 0$	$\chi = 9999$
0	720	1418.06	2128.58	974.67	1020.21	720	720
0.02	734.4	1446.42	2171.15	994.16	1040.61	734.4	734.4
0.04	748.8	1474.78	2213.72	1013.66	1061.01	748.8	748.8
0.06	763.2	1503.14	2256.29	1033.15	1081.42	763.2	763.2
0.08	777.6	1531.51	2298.86	1052.64	1101.82	777.6	777.6
0.1	792	1559.87	2341.43	1072.14	1122.23	792	792

Table 3
Variation of R_c and N_c for different $\delta,\ M_3$ and χ when $Bi=0$ and $\sigma=10$

δ	R_c ($N=0$)	N_c ($R=0$)					
		$M_3=1$		$M_3=10$		$M_3\to\infty$	
		$\chi=0$	$\chi=9999$	$\chi=0$	$\chi=9999$	$\chi=0$	$\chi=9999$
0	889.511	1782.43	2671.86	1222.77	1282.12	889.511	889.511
0.02	907.30	1818.08	2725.3	1247.22	1307.76	907.30	907.30
0.04	925.09	1853.73	2778.74	1271.68	1333.4	925.09	925.09
0.06	942.88	1889.37	2832.18	1296.13	1359.05	942.88	942.88
0.08	960.67	1925.02	2885.61	1320.59	1384.69	960.67	960.67
0.1	978.46	1960.67	2939.05	1345.04	1410.33	978.46	978.46

Table 4
Variation of R_c and N_c for different $\delta,\ M_3$ and χ when $Bi=1$ and $\sigma=10$

δ	R_c ($N=0$)	N_c ($R=0$)					
		$M_3=1$		$M_3=10$		$M_3\to\infty$	
		$\chi=0$	$\chi=9999$	$\chi=0$	$\chi=9999$	$\chi=0$	$\chi=9999$
0	1222.4	1969.9	2791.06	1402.23	1443.55	1222.4	1222.4
0.02	1246.85	2009.9	2846.88	1430.27	1472.42	1246.85	1246.85
0.04	1271.3	2048.69	2902.7	1458.31	1501.3	1271.3	1271.3
0.06	1295.75	2088.09	2958.52	1486.36	1530.17	1295.75	1295.75
0.08	1320.19	2127.49	3014.34	1514.4	1559.04	1320.19	1320.19
0.1	1344.64	2166.89	3070.16	1542.45	1587.45	1344.64	1344.64

4. Conclusions

The investigation focus is on the impact of MFD viscosity on the onset of Brinkman-Bénard ferroconvection in an ferrofluid-saturated porous layer, considering the variable viscosity of ferrofluid under an applied magnetic field. The porous layer is bounded by rigid-paramagnetic surfaces. The eigenvalue problem is numerically solved using the Galerkin technique with Rayleigh number R as the eigenvalue. The obtained results show excellent agreement with previously published works. The present study yields the following conclusions

i. The MFD viscosity parameter δ delays the onset of ferroconvection in the ferrofluid. This means that as the MFD viscosity parameter increases, it hinders the initiation of convection, making the system more stable and requiring higher values of critical Rayleigh number R_c for the convective motion to occur. The fluid's ability to flow becomes more resistant under the influence of the magnetic field, leading to a slower development of convection compared to the scenario without MFD viscosity.
ii. The effect of the magnetic number M_1 and nonlinearity of fluid magnetization parameter on R_c in ferrofluids indicates that increasing the magnetic number enhances the responsiveness of the fluid to the magnetic field, leading to a more efficient fluid flow and heat transfer. As a result, convection is triggered at lower thermal driving forces. Understanding this relationship can help in designing and optimizing magnetic fluid-based systems, where precise control of fluid motion and heat transfer is desired through magnetic fields.

iii. The critical thermal Rayleigh number (R_c) increases as both the Biot number Bi and porous parameter σ^2 increase, resulting in a delay in the onset of ferroconvection. This means that higher values of Biot number and porous parameter lead to a more stable system, requiring a higher critical Rayleigh number for the initiation of convection in ferrofluid-saturated porous layer.
iv. The system exhibits greater stability against ferroconvection when the boundaries are paramagnetic with a large magnetic susceptibility $(\chi \neq 0)$, compared to cases with very low susceptibility. The observation shows that $(R_c \text{ and } a_c)_{\chi\neq 0} > (R_c \text{ and } a_c)_{\chi=0}$.
v. As $M_3 \to \infty$, the results are reduced to those of the classical Rayleigh-Bénard problem due to the non-linearity of magnetization.
vi. Complementary effects are observed between the buoyancy and magnetic forces, with the system attaining greater stability in the presence of magnetic forces alone.

Acknowledgement
The authors gratefully acknowledge the financial assistance under Dr. AIT R & D Grant Scheme received from Panchajanya Vidya Peeta Welfare Trust and Dr. Ambedkar Institute of Technology, Bangalore for carrying out this work.

References
[1] Rosensweig, Ronald E. *Ferrohydrodynamics*. Courier Corporation, 2013.
[2] Gui, N. Gan Jia, C. Stanley, N-T. Nguyen, and G. Rosengarten. "Ferrofluids for heat transfer enhancement under an external magnetic field." *International Journal of Heat and Mass Transfer* 123 (2018): 110-121.https://doi.org/10.1016/j.ijheatmasstransfer.2018.02.100
[3] Senin, Nor Halawati, Nor Fadzillah Mohd Mokhtar, and Mohamad Hasan Abdul Sathar. "Chaotic convection in a ferrofluid with internal heat generation." *CFD Letters* 12, no. 10 (2020): 62-74. https://doi.org/10.37934/cfdl.12.10.6274
[4] Kole, Madhusree, and Sameer Khandekar. "Engineering applications of ferrofluids: A review." *Journal of Magnetism and Magnetic Materials* 537 (2021): 168222.https://doi.org/10.1016/j.jmmm.2021.168222
[5] Oehlsen, Oscar, Sussy I. Cervantes-Ramírez, Pabel Cervantes-Avilés, and Illya A. Medina-Velo. "Approaches on ferrofluid synthesis and applications: current status and future perspectives." *ACS Omega* 7, no. 4 (2022): 3134-3150.https://doi.org/10.1021/acsomega.1c05631
[6] Mahajan, Amit, and Mahesh Kumar Sharma. "Convection in magnetic nanofluids in porous media." *Journal of Porous Media* 17, no. 5 (2014).https://doi.org/10.1615/JPorMedia.v17.i5.60
[7] Nanjundappa, C. E., I. S. Shivakumara, and H. N. Prakash. "Effect of Coriolis force on thermomagnetic convection in a ferrofluid saturating porous medium: A weakly nonlinear stability analysis." *Journal of magnetism and magnetic materials* 370 (2014): 140-149. https://doi.org/10.1016/j.jmmm.2014.06.035
[8] Nanjundappa, C.E., Shivakumara, I. S., Arunkumar, R., and Tadmor, R. "Ferroconvection in a porous medium with vertical Throughflow." *Acta Mech* 226, (2015): 1515–1528. https://doi.org/10.1007/s00707-014-1267-1
[9] Gibanov, Nikita S., Mikhail A. Sheremet, Hakan F. Oztop, and Khaled Al-Salem. "Effect of uniform inclined magnetic field on natural convection and entropy generation in an open cavity having a horizontal porous layer saturated with a ferrofluid." *Numerical Heat Transfer, Part A: Applications* 72, no. 6 (2017): 479-494.https://doi.org/10.1080/10407782.2017.1386515
[10] Sheikhnejad, Yahya, Reza Hosseini, and Majid Saffar Avval. "Experimental study on heat transfer enhancement of laminar ferrofluid flow in horizontal tube partially filled porous media under fixed parallel magnet bars." *Journal of Magnetism and Magnetic Materials* 424 (2017): 16-25.https://doi.org/10.1016/j.jmmm.2016.09.098
[11] Qin, Y., and J. Chadam. "A nonlinear stability problem for ferromagnetic fluids in a porous medium." *Applied Mathematics Letters* 8, no. 2 (1995): 25-29.https://doi.org/10.1016/0893-9659(95)00005-B
[12] Borglin, Sharon E., George J. Moridis, and Curtis M. Oldenburg. "Experimental studies of the flow of ferrofluid in porous media." *Transport in Porous Media* 41 (2000): 61-80.https://doi.org/10.1023/A:1006676931721
[13] Shivakumara, I. S., C-O. Ng, and M. Ravisha. "Ferromagnetic convection in a heterogeneous porous medium." *Arabian Journal for Science and Engineering* 39 (2014): 7265-7274.https://doi.org/10.1007/s13369-014-1288-z

[14] Nanjundappa, C. E., I. S. Shivakumara, and R. Arunkumar. "Effect of cubic temperature profiles on ferro convection in a Brinkman porous medium." *Journal of Applied Fluid Mechanics* 9, no. 4 (2016): 1955-1962. https://doi.org/10.18869/ACADPUB.JAFM.68.235.24404

[15] Li, Zhixiong, Ahmad Shafee, M. Ramzan, H. B. Rokni, and Qasem M. Al-Mdallal. "Simulation of natural convection of Fe_3O_4-water ferrofluid in a circular porous cavity in the presence of a magnetic field." *The European Physical Journal Plus* 134 (2019): 1-8.https://doi.org/10.1140/epjp/i2019-12433-5

[16] Siddiqui, Abuzar Abid, and Mustafa Turkyilmazoglu. "Natural convection in the ferrofluid enclosed in a porous and permeable cavity." *International Communications in Heat and Mass Transfer* 113 (2020): 104499. https://doi.org/10.1016/j.icheatmasstransfer.2020.104499

[17] Senin, Nor Halawati, Nor Fadzillah Mohd Mokhtar, and Mohamad Hasan Abdul Sathar. "Ferroconvection in an anisotropic porous medium with variable gravity." *Journal of Advanced Research in Fluid Mechanics and Thermal Sciences* 71, no. 2 (2020): 56-68. https://doi.org/10.37934/arfmts.71.2.5668

[18] Nanjundappa, C. E., A. Pavithra, and I. S. Shivakuamara. "Effect of dusty particles on Darcy-Brinkman gravity-driven ferro-thermal-convection in a ferrofluid saturated porous layer with internal heat source: influence of boundaries." *International Journal of Applied and Computational Mathematics* 7 (2021): 1-20. https://doi.org/10.1007/s40819-020-00948-6

[19] Saeed, Munazza, Bilal Ahmad, and Qazi Mahmood ul Hassan. "Variable thermal effects of viscosity and radiation of ferrofluid submerged in porous medium." *Ain Shams Engineering Journal* 13, no. 4 (2022): 101653. https://doi.org/10.1016/j.asej.2021.101653

[20] Goyal, Komal, and Srinivas Suripeddi. "A note on two-fluid starting flow in a porous spaced channel with a magnetic field." *CFD Letters* 15, no. 9 (2023): 136-151. https://doi.org/10.37934/cfdl.15.9.136151

[21] Sunil, Divya, and R. C. Sharma. "The effect of magnetic field dependent viscosity on thermosolutal convection in a ferromagnetic fluid saturating a porous medium." *Transport in Porous Media* 60 (2005): 251-274. https://doi.org/10.1007/s11242-004-5739-y

[22] Nanjundappa, C. E., I. S. Shivakumara, and R. Arunkumar. "Bénard-Marangoni ferroconvection with magnetic field dependent viscosity." *Journal of Magnetism and Magnetic Materials* 322, no. 15 (2010): 2256-2263. https://doi.org/10.1016/j.jmmm.2010.02.021

[23] Bhandari, A. "Effect of magnetic field dependent viscosity on the unsteady ferrofluid flow due to a rotating disk." *International Journal of Applied Mechanics and Engineering* 25, no. 2 (2020): 22-39. https://doi.org/10.2478/ijame-2020-0018

[24] Molana, M., A. S. Dogonchi, T. Armaghani, Ali J. Chamkha, D. D. Ganji, and Iskander Tlili. "Investigation of hydrothermal behavior of Fe_3O_4-H_2O nanofluid natural convection in a novel shape of porous cavity subjected to magnetic field dependent (MFD) viscosity." *Journal of Energy Storage* 30 (2020): 101395. https://doi.org/10.1016/j.est.2020.101395

[25] Izadi, Mohsen, Masoud Javanahram, Seyed Mohsen Hashem Zadeh, and Dengwei Jing. "Hydrodynamic and heat transfer properties of magnetic fluid in porous medium considering nanoparticle shapes and magnetic field-dependent viscosity." *Chinese Journal of Chemical Engineering* 28, no. 2 (2020): 329-339. https://doi.org/10.1016/j.cjche.2019.04.024

[26] Savitha, Lakkanna, Chikkanalluru Erappa Nanjundappa, and Inapura Siddagangaiah Shivakumara. "Exploration of energy-based volumetric heating on ferrothermal porous convection: Effects of MFD viscosity and boundary conditions." *Heat Transfer* 51, no. 7 (2022): 6856-6872. https://doi.org/10.1002/htj.22627

[27] Rosensweig, R. E., R. Kaiser, and G. Miskolczy. "Viscosity of magnetic fluid in a magnetic field." *Journal of Colloid and Interface Science* 29, no. 4 (1969): 680-686. https://doi.org/10.1016/0021-9797(69)90220-3

[28] Finlayson, B. A. "Convective instability of ferromagnetic fluids." *Journal of Fluid Mechanics* 40, no. 4 (1970): 753-767. https://doi.org/10.1017/S0022112070000423

[29] Sparrow, Ephraim M., Richard J. Goldstein, and V. K. Jonsson. "Thermal instability in a horizontal fluid layer: effect of boundary conditions and non-linear temperature profile." *Journal of Fluid Mechanics* 18, no. 4 (1964): 513-528. https://doi.org/10.1017/S0022112064000386

[30] Gotoh, Kanefusa, and Michio Yamada. "Thermal convection in a horizontal layer of magnetic fluids." *Journal of the Physical Society of Japan* 51, no. 9 (1982): 3042-3048. https://doi.org/10.1143/JPSJ.51.3042